JOURNAL OF MATERIALS SCIENCE 26 (1991) 5445–5455

Fatigue limit and crack arrest in alkali-containing silicate glasses

E. GEHRKE*, Ch. ULLNER, M. HÄHNERT
Zentralinstitut für anorganische Chemie, D-1199 Berlin, Rudower Chaussee 5, FRG

Crack growth, including fatigue limit and crack arrest, have been investigated for glasses of the systems $x Na_2O$–$11 Al_2O_3$–$(89-x) SiO_2$, $x Na_2O$–$(100-x) SiO_2$ and $x Na_2O$–$7 CaO$–$(93-x) SiO_2$ in water as well as in acid and alkaline solutions. From studies of the dependence of the crack arrest on the alkali content of the glass, the kind of alkali (K^+, Na^+, Li^+), the pH of the corrosive medium, the ageing time and ageing loading in conjunction with measuring the alkali leaching behaviour, the basic mechanism of crack arrest and fatigue limit can be concluded. Owing to load- and medium-dependent diffusion processes, a crack-growth retarding leached layer at the crack is generated with modified strength and crack growth properties compared to the bulk properties. In high alkali-containing glasses the process is additionally stimulated by stresses produced in the leached layer at the crack tip and at the crack surfaces.

1. Introduction

The fatigue limit (or threshold load) is of special interest in the application of glass for structural components, in regard to both crack growth and fatigue. However, a precise determination of the fatigue limit is problematic because extremely small crack-growth velocities (10^{-8} to 10^{-12} m sec^{-1}) (or extremely long times-to-failure) must usually be measured. For this reason, knowledge of the basic mechanism resulting in the fatigue limit is relatively poor at present. For the case of alkali-containing silicate glasses, the slope of the crack-growth curve plotted as the logarithm of the crack velocity, ln v, against the stress intensity factor, K_I, varies at small velocities, $v < 10^{-7}$ m sec^{-1}. This effect indicates that the dominant mechanism is changed. In that range of crack velocity, surface corrosion processes and crack growth are superimposed at the crack tip. The two mechanisms are discussed generally to explain why the fatigue limit appears in those glasses. One mechanism is to assume crack-tip blunting as a result of network dissolution [1]. The other is to assume the generation of a crack-growth retarding layer due to alkali leaching [2].

Crack arrest is observed in some glasses after loading near the supposed fatigue limit, including corrosive attack at the crack tip [2–5]. Because crack arrest and fatigue limit should be based on the same mechanism, a study of crack arrest in detail will also provide more knowledge concerning the fatigue limit.

In this paper such studies are conducted on binary and ternary silicate glasses. By means of variations of the glass composition the different corrosion processes are stimulated and as a consequence, their influence on the crack arrest can be investigated.

2. Experimental procedure

The binary alkali silicate glasses and ternary alkali alumosilicate glasses, alkali borosilicate glasses, as well as alkali calcium silicate glasses, with different kinds of alkalies having different concentrations of alkali oxide (given in mol %) were melted in platinum crucibles. Al_2O_3 (1 mol %) was added to some of the binary glasses in order to reduce the phase-separation tendencies.

The annealed specimens of dimensions $75 \times 24 \times 2$ mm^3 (depth of the crack-guiding groove was 1 mm) were investigated using the double cantilever beam (DCB) method [6]. The crack-growth velocity was measured directly by means of an optical measuring microscope ($v < 10^{-3}$ m sec^{-1}) or indirectly using the modulation of the fracture surface generated by sound waves in burst mode ($v > 10^{-4}$ m sec^{-1}) [7, 8]. All of the obtained crack-growth curves have been plotted according to the function

$$v = v_0 \exp(\beta K_I) \quad (1)$$

where v is the crack-growth velocity and K_I the stress intensity factor.

For studying the crack arrest, the following procedure was applied. Assuming the value of the fatigue limit with regard to the crack growth curve is K_0, the specimen is loaded in water or other corrosive media at a stress intensity factor $K_A < K_0$ for the ageing time, t_A. Then the stress intensity factor is increased to $K_p > K_0$ and the crack propagation, Δa, is measured as a function of loading time, t_p. The experimental procedure, including the symbols used, is given in Fig. 1. Typical curves of crack propagation, Δa, measured, for instance, on a sodium alumosilicate glass are

* *Present address*: Fraunhofer-Institut für Werkstoffmechanik, Wöhlerstrasse 11, D-7800 Freiburg, FRG.

0022–2461/91 $03.00 + .12

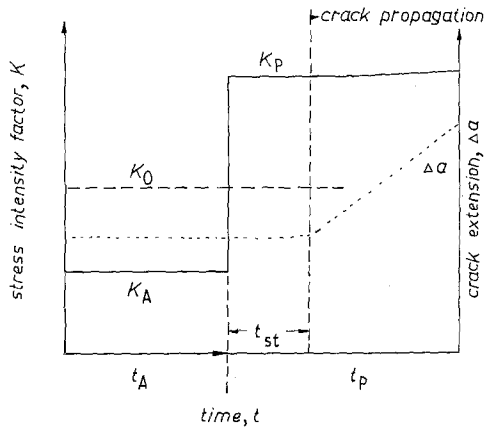

Figure 1 Experimental procedure for studying crack arrest.

shown in Fig. 2. The corrosive attack characterized by t_A and K_A is the same for all the curves in Fig. 2. By reason of the limited sensitivity of the measuring microscope only a crack extension $\Delta a \geqslant 10$ μm can be determined certainly. As shown in Fig. 2, the stable crack-growth velocity, which is equal to the velocity measured without previous corrosion attack, occurs only after a certain delay time, t_{st}, after increasing the crack loading from K_A to K_p. Thus, after corrosive attack at the crack tip the crack-growth velocity is not a unique function of the present stress intensity factor.

The delay time, t_{st}, is used as a scale for the effect of chemical interaction, because the moving crack front penetrates the modified region at the crack tip during that time. By comparing the effect of crack growth in different glasses and in different media the parameters K_A and t_A are found to vary. K_p is selected in every case in such a way that the resulting crack-growth velocity after penetrating the modified region ranges from $10^{-5} < v_p < 2 \times 10^{-5}$ m sec^{-1}.

For characterizing the corrosion behaviour of the investigated glasses, independent tests were conducted on rods in distilled water. The mass of alkali eluated from the glass was determined by means of an atom absorption method and plotted as a function of the corrosion time. After each measurement the test was continued in a fresh solution. So in respect of the pH of the solution, quasistatic conditions were approximately realized. At the beginning of corrosion the effective diffusion coefficient, D_{eff}, depends on the time, t, the leached mass of alkali, Q, and the alkali concentration in the volume, c_0, according to [9, 10]

$$D_{eff} = \frac{\pi}{4c_0^2}\left(\frac{Q}{t^{1/2}}\right)^2 \quad (2)$$

For stationary corrosion, the time dependence becomes [9]

$$Q/c_0 = y_{1/2} + v_{00}/t \quad (3)$$

So from the leaching rate, v_{00}, and the depth of the concentration profile at a concentration $c/c_0 = 0.5$, $y_{1/2}$ could be determined. Except for high alkali-containing glasses with poor water resistance, the stationary region of corrosion is reached only after more than 10^3 h. The ageing times chosen in crack-arrest experiments ranged from 20 to 60 min (maximum 72 h) lead to substantially smaller layer depths than the stationary value, $y_{1/2}$.

3. Results

3.1. Effect of load and time on crack arrest

First the fundamental effect of the parameters K_A and t_A is demonstrated on the system xNa$_2$O–11Al$_2$O$_3$–(89 – x)SiO$_2$. The crack-growth behaviour of these glasses containing 14, 26 or 36 mol % Na$_2$O, respectively, in water is shown in Fig. 3. In this system the fracture toughness decreases with increasing alkali content. The crack-growth curves are shifted to smaller values of K_I and the slope, β_1, of the curves in region 1 decreases. Every glass shows an evident transition from region 1 to the fatigue limit. With increasing alkali content the transition occurs at higher crack-growth velocities v_{01} (arrows, Fig. 3). The transition velocity, v_{01}, can be considered to be a scale for the corrosion activity to retard crack growth.

Next the load dependence of the crack arrest is demonstrated for the glass containing 26 mol % Na$_2$O. The crack tip is aged in water for $t_A = 60$ min or 16 h at different loadings, K_A, and the delay time, t_{st}, defined in Fig. 1 (bulk velocity $v_p = 1.5 \times 10^{-5}$ m sec^{-1}) is measured. As shown in Fig. 4 for $t_A = 60$ min, t_{st} rises poorly at low loads, K_A, and at higher loads a maximum can be observed. This maximum occurs exactly at the fatigue limit of the crack

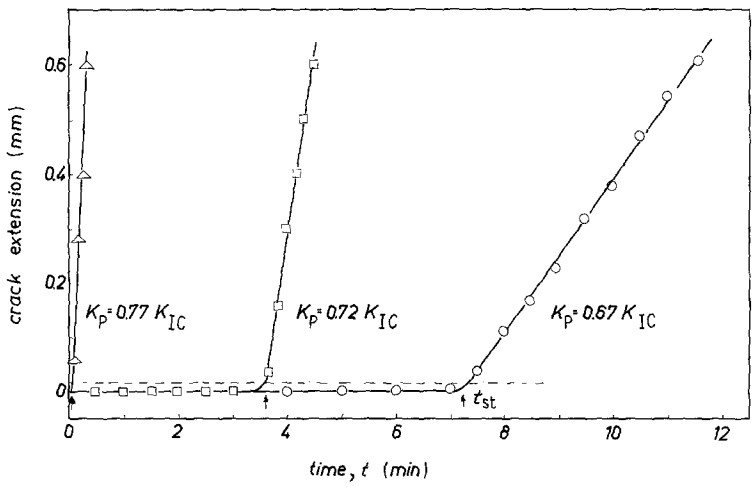

Figure 2 Crack extension after crack arrest under constant ageing conditions as a function of the loading time, t_P, for 26Na$_2$O–11Al$_2$O$_3$–63SiO$_2$ in water, $K_A = 0.57K_{IC}$, $t_A = 20$ min.

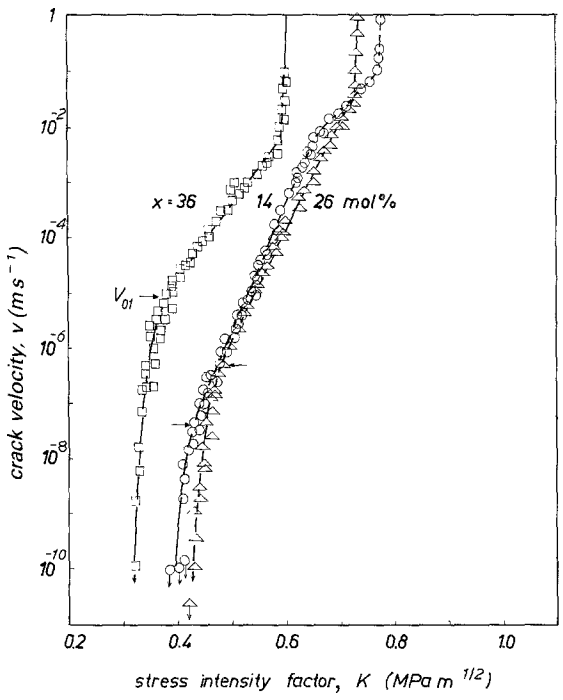

Figure 3 Crack growth curves of the system xNa_2O–$11Al_2O_3$–$(89 - x)SiO_2$ glasses in water.

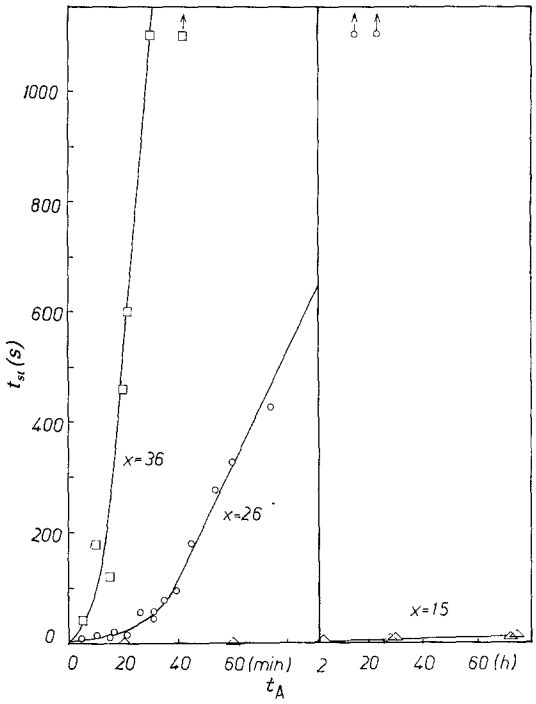

Figure 5 Dependence of the delay time, t_{st}, on the ageing time, t_A, at a load which nearly equals the fatigue limit, $K_A \approx K_0$, for sodium alumosilicate glasses with different Na_2O contents in water. $K_P = 1.5 \times 10^{-5}$ m sec^{-1}.

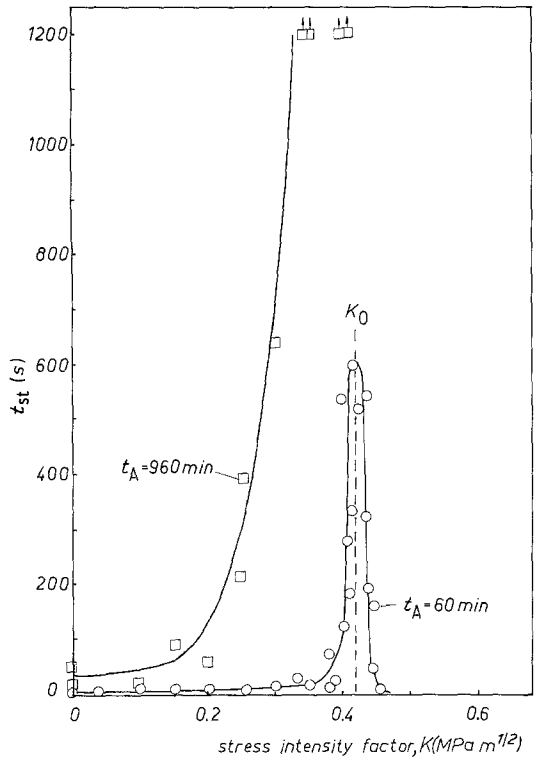

Figure 4 Dependence of the delay time, t_{st}, on the load, K_A, during the ageing period (t_A = constant) causing crack arrest for the glass $26Na_2O$–$11Al_2O_3$–$63SiO_2$ in water. $K_P = 1.0$ to 1.5×10^{-5} m sec^{-1}.

growth, K_0. Therefore, such experimental procedures can be used advantageously to determine the fatigue limit. For a higher corrosion time, t_A = 16 h, the crack arrest is more obvious.

The dependence of the crack arrest on ageing time, t_A, for $K_A \approx K_0$ is demonstrated in Fig. 5. It is shown that the crack arrest becomes more substantial with increasing Na_2O content. This effect correlates to the transition velocity of the crack growth (Fig. 3) which depends on the Na_2O content in the same way. So the influence of the same mechanism is confirmed. As also shown in Fig. 5, the time dependence of the crack arrest expressed by t_{st} corresponds neither to t nor to $t^{1/2}$. Instead, t_{st} rises slowly at the beginning and more rapidly afterwards.

3.2. Crack arrest in alkali-free alumosilicate glasses

For comparison, the crack growth of alumosilicate glasses containing either Na_2O or CaO at the same concentration (26 mol %) is shown in Fig. 6. Although the sodium oxide-containing glass has a higher toughness, the crack-growth behaviour is the same at velocities between 10^{-6} and 10^{-2} m sec^{-1}. However, typical differences can be seen in the range of smaller crack-growth velocities. The sodium oxide-containing glass shows a substantial fatigue limit, whereas the crack-growth curve of the CaO-containing glass diminishes as a straight line up to 10^{-10} m sec^{-1}. Thus crack-growth retarding processes do not occur in the last glass. A fatigue limit might occur only below 0.36 MPa m$^{1/2}$.

Corresponding studies, such as those carried out on the sodium oxide-containing glass (Figs 4 and 5), do not result in any crack arrest at loads ranging from $0.28 < K_A < 0.38$ MPa m$^{1/2}$, even for ageing times up to 64 h. This essential result shows that the existence of slightly leachable alkali ions is the fundamental condition for the occurrence of the crack arrest.

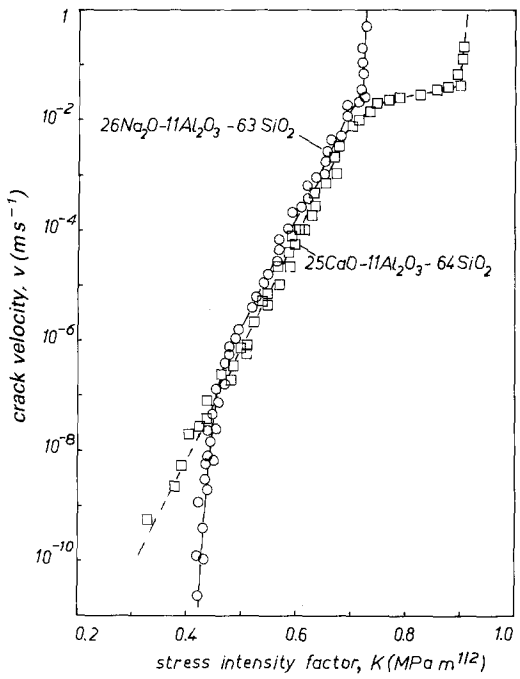

Figure 6 Effect of different leaching behaviour of the glasses $26Na_2O$–$11Al_2O_3$–$63SiO_2$ and $26CaO$–$11Al_2O_3$–$63SiO_2$ on the crack growth in water at 23 °C over the range of fatigue limit.

3.3. Effect of the pH of the environment

As is known, certain media can enhance (0.1N HCl, pH = 1) or diminish (0.1N NaOH, pH = 12) the interdiffusion between alkali ions of the glass and protons or hydrogenium ions of the medium in comparison to distilled water (pH = 6). On the other hand, the dissolution rate of the network rises with increasing pH of the medium [11, 12]. But how is the crack arrest influenced by those media?

The crack growth of the $26Na_2O$–$7Al_2O_3$–$67SiO_2$ glass in those media is similar above 10^{-7} m sec^{-1} (Fig. 7). Below this velocity a transition to the fatigue limit is evident in water and acid media. In the alkaline media a shift to smaller K_I is observed.

The media effect on the crack arrest is shown in Fig. 8. For an ageing time of 60 min the effect is enhanced by the acid media in comparison to water, but in the alkaline media the crack arrest is too small to be measured ($t_{st} < 1$ sec). This is in line with the assumption that the crack arrest is caused by alkali leaching. So we can conclude that at the crack-tip area a leached layer is formed with mechanical properties modified in relation to the bulk properties and effects as a crack-growth barrier. The interdiffusion process is load dependent, evidently, as is demonstrated in Figs 4 and 8. An enhanced process of crack-growth hindrance with decreasing pH of the medium is observed in alkali-containing glasses, including commercial glasses (soda-lime glass or borosilicate glass [13, 14]) except some glasses with very high alkali contents, as can be concluded from Table I. A glass such as $26Na_2O$–$11Al_2O_3$–$63SiO_2$ shows the crack growth plotted in Fig. 9. Above 10^{-6} m sec^{-1} there are small differences in alkaline, neutral and acid media again, but at smaller crack-growth velocities a plateau-like region is formed in acid media (called region O′). Michalske and Bunker [15] found an analogous behaviour in $30Na_2O$–$10B_2O_3$–$60SiO_2$ glass in 0.5 and 5N HCl. They discussed the effect by assuming tensile stresses in the leached layer at the crack tip.

From crack-arrest studies on glasses such as $26Na_2O$–$11Al_2O_3$–$63SiO_2$, the delay time, t_{st}, is found to be less than 1 sec after an ageing time < 1 h, and after t_A = 72 h in 0.1N NaOH, t_{st} is also less by two to three orders of magnitudes compared to the delay time measured in water (Fig. 5).

In 0.1 and 1N HCl, crack arrest is too small to be measured although the layer formed is enhanced in

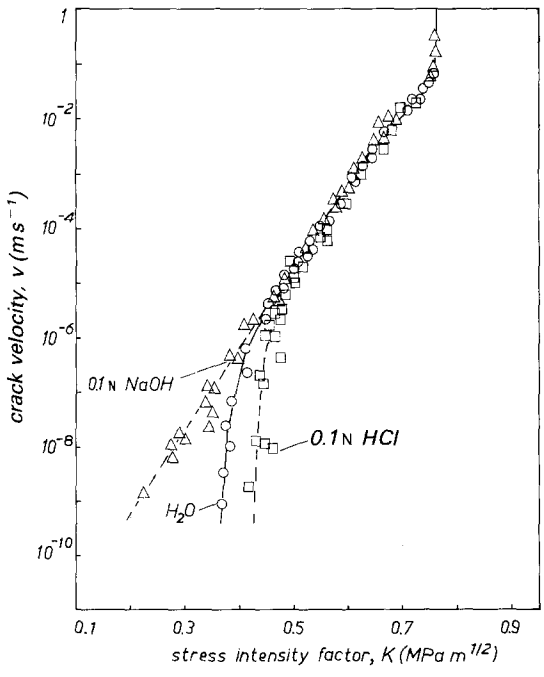

Figure 7 Effect of the corrosion medium on the crack growth of the $26Na_2O$–$7Al_2O_3$–$67SiO_2$ glass over the range of fatigue limit.

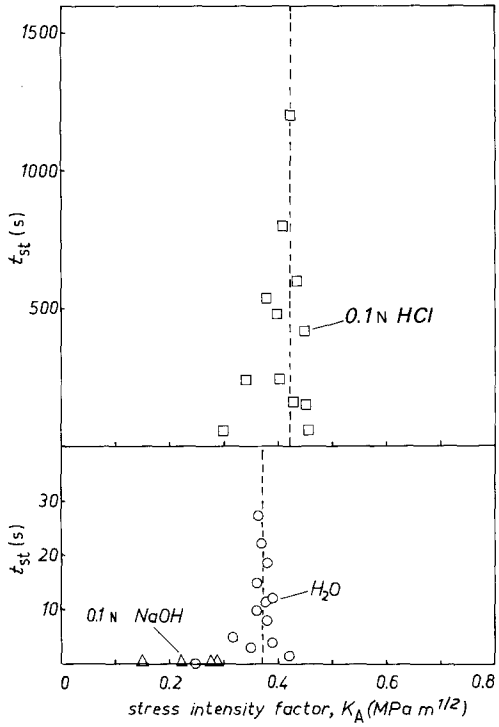

Figure 8 Crack arrest in the $26Na_2O$–$7Al_2O_3$–$67SiO_2$ glass on ageing in water and hydrochloric acid for 60 min as a function of the load, K_A.

TABLE I Effect of the corrosion medium on the crack arrest (delay time, t_{st}), the fatigue limit (stress intensity factor, K_0) and the transition velocity (v_{01}) of silicate glasses

Glass composition (mol %)	Medium	$K_A = K_0$	t_{st} (sec)		v_{01}
		(MPa m$^{1/2}$)	t_A = 1 h	t_A = 16 h	(m sec^{-1})
$17Na_2O$–$11Al_2O_3$–$72SiO_2$	1N NaOH	0.35	< 1	< 1	1×10^{-8}
	H_2O	0.40	5	65	1×10^{-7}
	1N HCl	0.43	70	2070	5×10^{-7}
$26Na_2O$–$11Al_2O_3$–$63SiO_2$	0.1N NaOH	0.40	< 1	5	1×10^{-7}
	H_2O	0.42	600	> 3600	5×10^{-7}
	0.1N HCl	region O′	–	–	(2×10^{-7})
$17Na_2O$–$11B_2O_3$–$72SiO_2$	1N NaOH	0.28	< 1	< 1	5×10^{-9}
	H_2O	0.33	< 1	10	5×10^{-8}
	1N HCl	0.36	25	2100	1×10^{-7}
$28Na_2O$–$11B_2O_3$–$61SiO_2$	1N NaOH	< 0.30	< 1	< 1	$< 10^{-9}$
	H_2O	0.36	< 1	5	2×10^{-8}
	1N HCl	region O′	–	–	(5×10^{-7})
$17Na_2O$–$83SiO_2$	1N NaOH	< 0.28	< 1	5	1×10^{-8}
	H_2O	0.35	35	> 3600	3×10^{-7}
	1N HCl	0.46	> 3600	> 3600	1×10^{-5}
$24Na_2O$–$76SiO_2$	1N NaOH	region O′	–	–	(2×10^{-6})
	H_2O	0.28	10	18	2×10^{-7}
	1N HCl	0.41	> 3600	–	2×10^{-6}
$17Na_2O$–$7CaO$–$76SiO_2$	1N NaOH	< 0.26	< 1	3	1×10^{-8}
	H_2O	≤ 0.32	< 1	7	2×10^{-7}
	1N HCl	0.40	15	210	1×10^{-6}
$27Na_2O$–$7CaO$–$66SiO_2$	1N NaOH	< 0.36	< 1	< 1	2×10^{-8}
	H_2O	0.38	6	120	2×10^{-7}
	1N HCl	0.46	> 3600	> 3600	2×10^{-6}

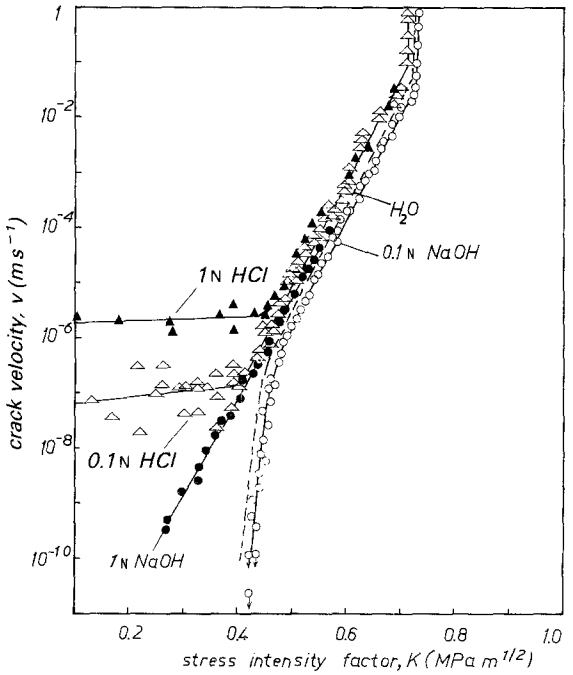

Figure 9 Crack growth of the $26Na_2O$–$11Al_2O_3$–$63SiO_2$ glass in different corrosive media.

comparison to water. Obviously not only the layer depth but also other properties of the layer, such as increasing tensile stress, are important for crack arrest. The leaching behaviour of this glass is increased by a factor of five in comparison with the glass in Figs 7 and 8.

The results collected in Table I allow more general conclusions to be drawn regarding the media effect of the crack arrest in glass. Binary sodium silicate glasses and ternary sodium borosilicate glasses are included. The crack arrest is measured at the load $K_A = K_0$ for different ageing times, t_A = 1 and 16 h. Sodium borosilicate glasses always show a smaller crack arrest in water than analogous alumosilicate glasses. In sodium calciumsilicate glasses, the crack arrest is also relatively small.

In principle, in glasses with slight or medium leaching behaviour the crack arrest is enhanced with decreasing pH of the media. This enhancement, which retards the crack growth, is also expressed by increasing transition velocity, v_{01}, in the crack-growth curves. In this way the experimental fatigue limit, K_0, is also increased. Therefore, the fatigue limit is dependent on the medium and must not be considered as a material parameter.

The different behaviour of some alumosilicate glasses and some borosilicate glasses with high alkali contents in acid media is related to the formation of thicker layers. So the enhanced transformation of the network structure leads to stresses stimulating crack growth.

3.4. Effect of the kind of alkali ions

The effect of the kind of alkali ions on the crack-growth behaviour is demonstrated by the glass system $26Me_2O$–$11Al_2O_3$–$63SiO_2$ in Fig. 10. The fracture toughness increases and the slope in region 1, β_1,

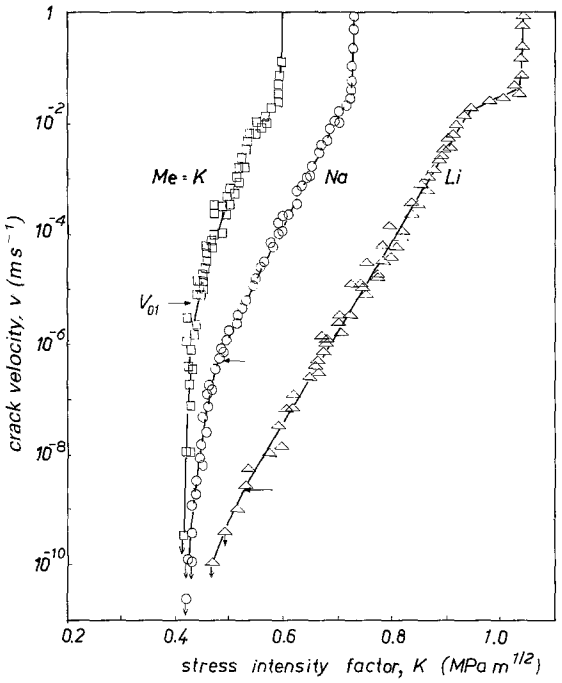

Figure 10 Effect of the kind of alkali ions (Me) in the system $26Me_2O$–$11Al_2O_3$–$63SiO_2$ on the crack growth in water.

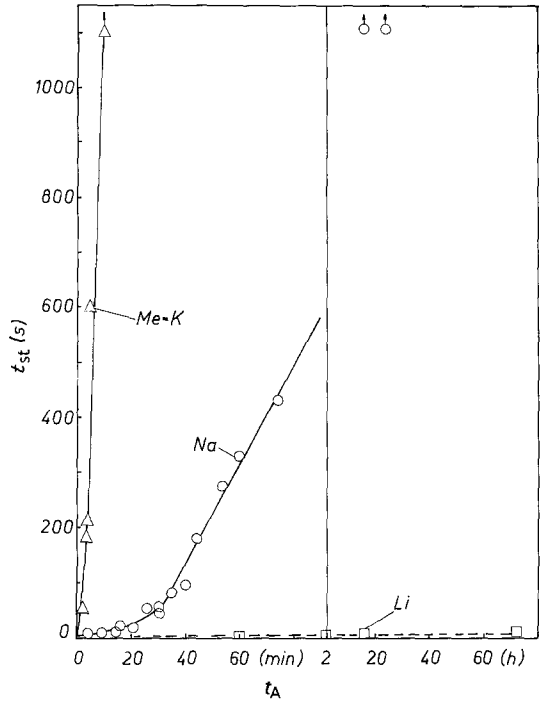

Figure 11 Effect of the kind of alkali ions (Me) in the system $26Me_2O$–$11Al_2O_3$–$63SiO_2$ on the crack arrest in water. $K_A \approx K_0$, $K_P = 1.5 \times 10^{-5}$ m sec^{-1}.

decreases with increasing field strength of the cation, in the order potassium, sodium, lithium. The transition velocity, v_{01}, from region 1 to the region of the fatigue limit (indicated by arrows in Fig. 11) is reduced in the same order in accordance with decreasing leaching ability of the glasses (conducted corrosion experiments on glass rods are given in Table II).

The crack arrest of the glasses, measured always at $K_A \approx K_0$, is plotted as a function of ageing time, t_A, in Fig. 11. The effect becomes stronger with increasing leaching ability of the glasses in the order lithium, sodium, potassium. It is interesting that only poor crack arrest can be observed in the lithium oxide-containing glass, even at extended ageing times up to 72 h. On the other hand, a substantial layer generation can be concluded from corrosion experiments for the lithium oxide-containing glass. So this result confirms how important are the specifically different structure of the glass and the properties of the leached layer formed for crack arrest.

TABLE II Data on the corrosion of the investigated glasses in distilled water at 23 °C

Glass composition (mol %)	Corrosion parameter		
	Initial state	Steady state	
	D_{eff} (m^2 sec^{-1})	$y_{1/2}$ (m)	V_{00} (m sec^{-1})
xNa_2O–$(100 - x)SiO_2$			
$x = 12$	5.4×10^{-19}	9.9×10^{-7}	1.4×10^{-14}
17	1.8×10^{-17}	6.2×10^{-6}	6.8×10^{-14}
24	8.8×10^{-17}	1.9×10^{-5}	4.1×10^{-12}
36	1.2×10^{-15}	2.3×10^{-5}	4.5×10^{-10}
xNa_2O–$11Al_2O_3$–$(89 - x)SiO_2$			
$x = 14$	1.2×10^{-21}	6.6×10^{-8}	1.2×10^{-15}
17	1.5×10^{-21}	–	–
26	6.0×10^{-21}	3.2×10^{-7}	1.6×10^{-14}
36	8.5×10^{-19}	5.4×10^{-7}	1.2×10^{-13}
$26Me_2O$–$11Al_2O_3$–$63SiO_2$			
Me = Li	1.5×10^{-21}	1.2×10^{-7}	2.6×10^{-15}
K	1.5×10^{-19}	4.7×10^{-6}	2.6×10^{-13}
xNa_2O–$11B_2O_3$–$(89 - x)SiO_2$			
$x = 17$	6.8×10^{-22}	3.9×10^{-8}	9.8×10^{-16}
28	1.6×10^{-17}	4.9×10^{-6}	5.0×10^{-12}
xNa_2O–$7CaO$–$(93 - x)SiO_2$			
$x = 17$	2.9×10^{-19}	–	–
28	1.5×10^{-18}	2.9×10^{-6}	1.5×10^{-13}

3.5. Crack arrest in binary silicate glasses

Crack growth in binary silicate glasses with different sodium oxide contents, x, including silica glass, $x = 0$, is demonstrated in Fig. 12. The behaviour in the range of smaller crack-growth velocities is of particular interest with regard to the chemical durability or the leaching ability, respectively. A unique mechanism of crack growth (without any evident fatigue limit) works in silicate glass down to 10^{-10} m sec^{-1}, whereas with increasing sodium content the typical transition to the fatigue limit can be observed first at 24 mol % Na_2O. At higher Na_2O contents (> 30 mol %) a plateau-like 0′ region appears. This means that the crack also propagates at the smallest stress intensity factors. The region 0′, also observed by Simmons and Freiman [5] can be related unambiguously to the crack growth, due to stress-dependent network dissolution including experimentally proved crack-tip blunting [16]. The crack-growth velocity extrapolated to $K = 0$ corresponds to the dissolution rate, v_{00}, measured on glass rods (Table II).

Crack arrest, including the strong dependence of the transition time, t_{st}, on the loading, K_A, is also observed in binary silicate glasses (Fig. 13). However, there is an essential difference concerning the dependence of the sodium content compared to the behaviour of the sodium alumosilicate glasses. The transition time, t_{st}, measured at $K_A \approx K_0$ and plotted in Fig. 14 as a function of ageing time, t_A, shows that the influence of crack-growth retarding processes is reduced with increasing alkali content, despite the increasing depth of the leached layers, and contrary to the effect of alkali content in sodium alumosilicate glasses (Fig. 5).

In every case the crack arrest is much more obvious in glasses with 12, 17 and 24 mol % Na_2O than in glasses with higher sodium content (36 mol %) in which the crack-tip blunting, due to network dissolution, can be observed directly [16, 17]. Because the dissolution rate, v_{00}, of those glasses increases with increasing sodium content (Table II) the crack-tip blunting cannot be considered to be the dominant mechanism for crack arrest. Instead, crack arrest is caused mainly by the formation of a leaching layer. Comparing crack arrest in different glass systems, this layer can both retard or stimulate the crack growth, depending on the glass composition.

4. Discussion

In principle, it is assumed that layer generation occurs at the crack tip as well as on the crack surfaces. First studies of crack generation resistance of corroded glass surfaces tested under Vickers indentation load confirm that the mechanical properties of the leached layers are different from the properties of the fresh surface, depending on the glass composition.

Although the relation between layer generation and crack arrest is evident, the complexity of running corrosion processes makes the connection between the measuring values t_{st} with certain properties of the layer more difficult. The following different mechanism could determine crack arrest, both in single or mixed mode.

4.1. Mechanism A: increased toughness/ crack-growth resistance

The crack-growth resistance and the toughness of the surface layer modified chemically is higher than the bulk material. In this area, alkali ions are replaced by protons and molecular water penetrates into the holes of the silicate network [18, 19]. As has already been shown in Fig. 10, the kind of cations bounded at nonbridging oxygens essentially influences the toughness and the crack growth. The toughness increases

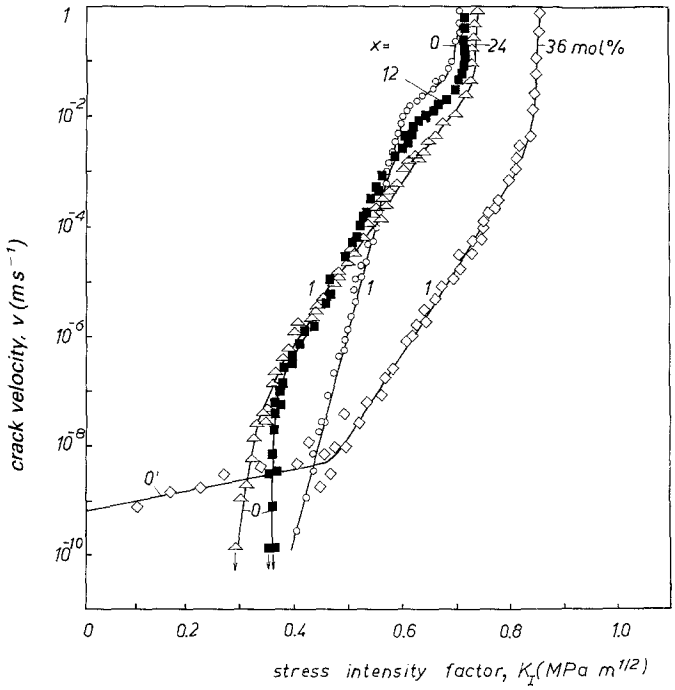

Figure 12 Crack growth of binary sodium silicate glasses in water at 23 °C.

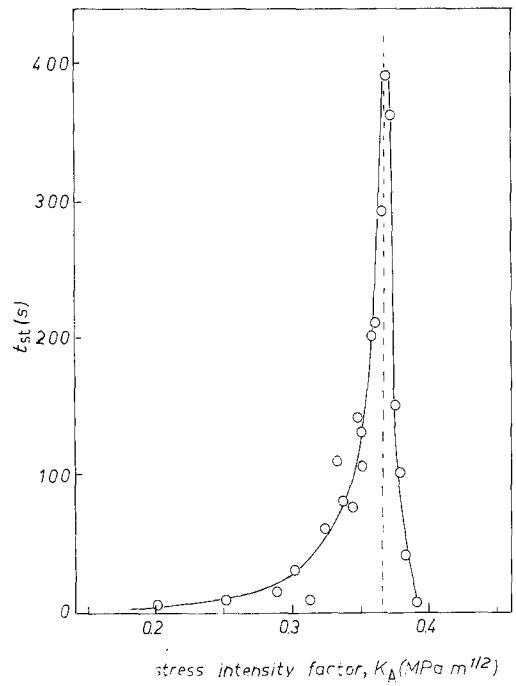

Figure 13 Crack arrest in the $12Na_2O$–$1Al_2O_3$–$87SiO_2$ glass in water at 23 °C (see Fig. 4). $t_A = 60$ min, $K_P = 1.2 \times 10^{-5}$ m sec^{-1}.

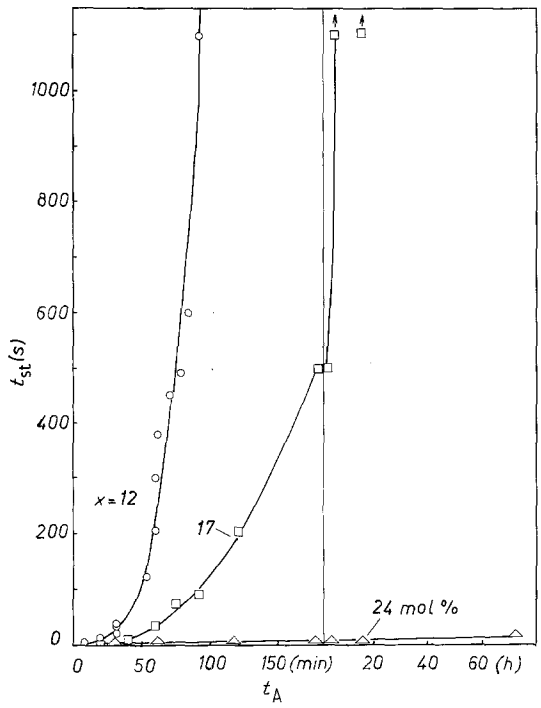

Figure 14 Effect of the Na_2O content on crack arrest in xNa_2O–$(100 - x)SiO_2$ in water (see Fig. 5). $K_A \approx K_0$, $K_P \approx 1.2 \times 10^{-5}$ m sec^{-1}.

with decreasing cation radius, and thus with increasing field strength of the cations. The question arises whether the insert of protons with an ionic radius less than one of the alkalies and with an increased field strength, can cause analogous effect?

Studies of the ageing effect of mechanically damaged glasses with a similar composition on the inert strength and dynamic fatigue seem to confirm such a theory. The observed strength enhancement after corrosive attack correlates temporally to the initial state of leaching process expressed by the leaching profile of alkali ions. The maximum enhancement attainable of the inert strength increases in the order lithium, sodium, potassium at the same alkali content [20, 21]. Thus the higher the difference between the field strengths of the leached alkali ions and the incorporated protons, the higher is the strength enhancement. The effect is increased with increasing absolute content of alkali oxides in the glass. In the same way, the strength level of transition to the fatigue limit in dynamic fatigue experiments is increased. Also the effect of increasing fatigue limit becomes stronger in the sequence lithium, sodium, potassium and with increasing alkali content.

4.2. Mechanism B: stress build-up

The volume of the surface layer is modified by the leaching process. Thus the effective stress intensity factor is influenced by a contribution of the layer, K_L

$$K_R = K_p + K_L \quad (4)$$

The crack arrest is stimulated by a negative K_L (pressure) whereas a positive K_L (tensile) leads to a weakness, in extreme cases up to spontaneous crack growth.

Crack arrest caused by generated pressure as a consequence of the ion exchange only is improbable, because protons with smaller radius occupy the positions of alkali ions in the glass. Stresses should be generated by the rearrangement of the glass network due to OH^- ions produced during the ion exchange or due to water diffused into the glass during the advanced leaching process with increasing layer depth. The breakage of silixane bondings (hydrolyse) and the enhanced incorporation of water can lead to an increasing volume and therefore to pressure. If such processes happen on the crack surface, the pressure in the layer can increase indirectly the stress intensity factor, K_R. On the other hand, tensile stress can be generated in the layer by condensation of neighbouring silanol groups (repolymerization) [10, 18, 22].

Evidence of the generated stresses is given by the appearance of the region O′ in some high alkali-containing glasses in certain media. The velocity of region O′ extrapolated to $K = 0$ is greater by four to eight magnitudes than the dissolution rate measured on glass rods (Fig. 9 and Table I). Thus material being removed from the surface, as happens in binary silicate glasses with 36 mol % alkali oxide (Fig. 12), cannot cause the region 0′ to form.

Crack generation and bursting of the corroded layer observed at certain high alkali-containing glasses indicate the presence of tensile stresses [10]. Michalske and Bunker [15] measured surface stresses on sodium borosilicate glasses ($30Na_2O$–$10B_2O_3$–$60SiO_2$) corroded in HCl using an interferometric method. First pressure stress is generated in 0.5N HCl, but after a longer corrosion time the stress was changed to tensile stress. In contrast, only tensile stresses are generated in 5N HCl. The crack-growth curves of a glass with the same composition in HCl shows a typical region 0′

(Fig. 9 and Table I) which is correlated to the tensile stress in the layer.

Measurements of the crack-generation resistance under Vicker's pyramid loading on the same glass also indicate the generation of tensile stresses after corrosion in HCl. In the same way, tensile stresses exist at the surface of binary glasses with high alkali content after corrosion in water. On studying the inert strength of the corroded binary silicate glasses, a strength maximum was found during the initial state of corrosion. For longer corrosion times, the inert strength falls off below the initial strength of the fresh specimens. The decrease of the inert strength becomes stronger with increasing alkali content and can evidently be related to the stress generation in the corrosion layer [20]. By analogy, the reduction of the crack arrest in binary silicate glasses with increasing sodium oxide content can be explained (Fig. 14).

4.3. Mechanism C: blunting of the effective crack-tip geometry

The leached layer is "softer" due to enhanced plastic deformation. So blunting of the effective crack-tip geometry leads to a decrease in the effective loading at the crack tip [23].

If this theory is suitable, the crack arrest would be enhanced on increasing the thickness of the layer and on decreasing the hardness. In contrast, the experimental results on sodium silicate glasses, sodium borosilicate glasses and lithium alumosilicate glasses with high alkali content show that there is no or only a slight effect of crack arrest, although the layer thickness is substantial and a reduction in hardness was proved for some glasses.

4.4. Mechanism D: interface forces due to corrosion products

Corrosion products form layers at the crack surface near the crack tip. Lawn and co-workers [24, 25] concluded from investigations of the crack growth and strength on mica, silica glass and soda-lime glass, that after a corrosive attack these layers lead to a "bridging" between the crack surfaces and this effects crack growth retardation or strength enhancement, respectively.

However, such forces cannot play an important role in crack arrest because the experimental results show that this does not appear in silica glass and alkali free alumosilicate glasses, even after advanced ageing in water. If the interface forces formed by corrosion products are dominant, the re-opening of the healed cracks would require a higher stress intensity factor after corrosive attack in water than after ageing in air. The experimental results given by Stavrinides and Holloway [26] on silica glass, sodiumborosilicate glass and soda-lime glass, show exactly the opposite effect.

According to the experimental results, mechanisms C and D only seem to play a lesser role for crack-growth retarding processes. When mechanism A is the basic mechanism of crack arrest, this effect should be stimulated additionally by mechanism B. The two mechanisms can be effective at different depths of the leached layer. The stress generation should occur mainly in the structurally disturbed near-surface zone of the layer.

What happens after crack arrest finishes on incrementally increasing the stress intensity factor from K_A to K_p (Fig. 1)? For all four mechanisms it can be assumed that the crack front passes through the corroded layer of thickness Δa_L with the modified median crack-growth velocity of the layer during the transition time, t_{st}.

$$v_L \approx \Delta a_L / t_{st} \tag{5}$$

The velocity, v_L, depends on the ageing conditions, t_A, K_A, and on the loading K_p at the following crack propagation. In particular, v_L is influenced by the modified material properties in the leached layer. The thickness a_L is only a function of t_A and K_A. Assuming for v_L a crack-growth function such as Equation 1 and constant corrosion conditions, t_A, K_A, it follows that

$$v_L \approx \Delta a_L / t_{st} = v_{L0} \exp(\beta_L K_p) \tag{6}$$

Equation 6 is valid for constant corrosion conditions, t_A, K_A, and constant properties inside the leached layer characterized by the parameters v_{L0}, β_L. If Equation 6 is suitable, there must be a straight line with the slope β_L in the diagram plotted with $\ln(t_{st-1})$ against K_p. Fig. 15 demonstrates the dependence of the transition time, t_{st}, on the loading, K_p, at constant ageing conditions (in water at $K_A \approx K_0$, $t_A = 10$ and 20 min, respectively) by a sodium alumosilicate glass ($26Na_2O$–$11Al_2O_3$–$63SiO_2$). Also, for other glasses, straight lines represent the dependence. The calculated slopes, β_L, are collected in Table III. Comparing the slopes of the leached layer, β_L, with those of the bulk material, β_V, the parameter β_L is essentially greater than β_V and ranges by the magnitude of silica glass

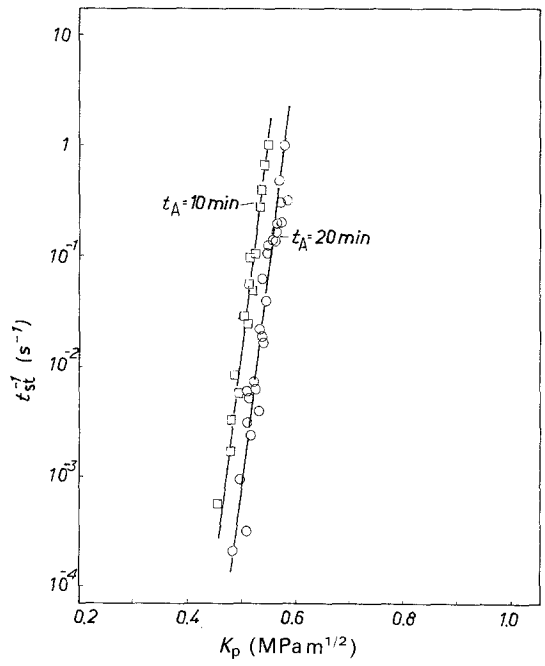

Figure 15 Dependence of the reciprocal delay time, t_{st}^{-1}, on the load, K_p, during the crack extension after crack arrest ($K_A \approx K_0$, t_A = constant), in $26Na_2O$–$11Al_2O_3$–$63SiO_2$ in water.

($\beta_V = 81.4$ MPa $m^{1/2}$). Thus the effective part of the leached layer leads to load dependence of the crack growth, comparable to silica glass. On the other hand, it can be concluded from Table III that the effective part of the leached layer for all the glass systems investigated has similar properties concerning crack growth. Therefore, this part of the leached layer is related to the "neutralization zone" located between the "transformation zone" and the bulk. According to Wigby [27], who performed measurements of the electrical conductivity on layer-by-layer etched glass surfaces after corrosion, the neutralization layer is almost free of mobile cations. But stresses should be generated in the "transformation zone", the structure of which is strongly disturbed [22].

The process of crack propagation after crack arrest is still relatively clear (Equation 6) whereas the dependence of the generation of the crack-growth retarding layer on t_A and K_A is very hard to describe by a quantitative model. The measured value of t_{st} is determined by the effective layer thickness, Δa_L, and the crack-growth velocity, v_L, in the layer. The two values are functions of t_A and K_A. Without considering the crack growth, the time dependence of the effective layer thickness is approximately

$$\Delta a_L \sim \Delta a_{L^*} = \text{constant } (D_{eff} t)^{1/2} \quad (7)$$

The profile depth, Δa_{L^*} is defined by the relative alkali concentration $c/c_0 = 0.5$ [9]. The effective diffusion coefficient of the alkali ions, D_{eff}, is expected to be load dependent. Nogami and Tomozawa [28] used an exponential dependence on the hydrostatic pressure, p, for the diffusion of water into silica glass. Applied to the present problem the load dependence gives

$$D_{eff} = D(K_A = 0) \exp[AK_A] \quad (8)$$

Parameter A is independent of loading
From Equations 8 and 5 we obtain

$$t_{st} = \text{constant } \frac{D(c)^{1/2} t_A^{1/2}}{v_L} \exp[AK_A/2] \quad (9)$$

Such a dependence of the transition time, t_{st}, on t_A and K_A is not observed (see the Figs 5, 11, 14 and 4, 13, respectively), because during the transition period the crack-growth velocity in the layer, v_L, as a scale for the modification of the layer property, also varies with t_A and K_A. Thus for improved modelling it is necessary to characterize the layer properties using further methods.

However, the load dependence of the crack arrest is evident proof that a leached layer must be generated even during crack propagation, because crack arrest also occurs above the fatigue limit, K_0. The transition velocity of the crack growth curve, v_{01}, indicates the maximum velocity at which an effective layer with modified properties can be formed.

$$\frac{\Delta a_L}{\Delta t}(K_I) \geqslant \frac{\Delta a}{\Delta t}(K_I) \quad \text{for } K_I \leqslant K_I(v_{01}) \quad (10)$$

A five- or fifteen-fold increase in the leaching rate using different media with pH = 12 (NaOH), pH = 6 (H_2O) and pH = 1 (HCl) [11–13] produces an increase in the transition velocity, v_{01}, in the same way.

5. Conclusions

1. Both crack arrest and transition to the fatigue limit of the crack-growth curve are based on the same mechanism, namely the generation of a leaching layer at the crack tip due to interdiffusion between alkali ions of the glass and water-containing species (H_3O^+, H_2O) of the medium (Figs 3 to 12).

2. The diffusion process is load dependent and also occurs when the crack tip is moving ($K_A > K_0$, Figs 4, 8, 13).

3. Not only the depth of the layer but also the special mechanical properties are of essential importance.

4. As demonstrated especially on binary silicate glasses (Fig. 14), the crack-tip blunting due to network dissolution cannot be considered to be a dominant mechanism, contrary to reports in other papers [4, 17].

Mechanism A (increased toughness/crack-growth resistance) seems to be the basic mechanism of crack arrest. Mechanism A should be stimulated additionally by mechanism B (stress build-up).

TABLE III Comparison of the crack growth parameters, β_L (of the leached layer) and β_V (of the bulk material)

Glass composition (mol %)	Medium	t_A (min) (by $K_A \approx K_0$)	β_L (MPa $m^{1/2})^{-1}$	β_V (MPa $m^{1/2})^{-1}$
xNa_2O–$(100-x)SiO_2$	H_2O	60		
$x = 12$	H_2O	60	80.9	41.9
17	H_2O	30	76.8	33.6
24	H_2O	30	57.6	35.0
xNa_2O–$11Al_2O_3$–$(89-x)SiO_2$				
$x = 21$	H_2O	120	83.1	47.0
26	H_2O	20	86.3	41.4
36	H_2O	20	88.1	35.9
xNa_2O–$11B_2O_3$–$(89-x)SiO_2$				
$x = 17$	1N HCl	60	95.9	34.9
22	0.1N HCl	15	79.1	34.4
xNa_2O–7CaO–$(93-x)SiO_2$				
$x = 17$	1N HCl	60	75.5	37.4
27	1N HCl	20	90.8	26.8

Acknowledgement

The authors thank Monika Finn for conducting the crack growth measurements so carefully.

References

1. W. B. HILLIG and W. B. CHARLES, in "High Strength Materials", edited by V. F. Zackey (Wiley, New York, 1965) p. 682.
2. E. GEHRKE and CH. ULLNER, *Adv. Ceram.* **22** (1988) 77.
3. S. M. WIEDERHORN and H. JOHNSON, *J. Amer. Ceram. Soc.* **56** (1973) 192.
4. T. A. MICHALSKE, in "Fracture Mechanics of Ceramics", Vol. 5, edited by R. C. Bradt, D. P. H. Hasselman and F. F. Lange (Plenum, New York, 1983) p. 277.
5. C. J. SIMMONS and S. W. FREIMAN, *J. Amer. Ceram. Soc.* **64** (1981) 683.
6. S. M. WIEDERHORN, *ibid.* **50** (1967) 407.
7. H. RICHTER, *Glastechn. Berichte* **56K** (1983) 402.
8. E. GEHRKE, CH. ULLNER and M. HÄHNERT, *ibid.* **60** (1987) 268.
9. R. H. DOREMUS, in "Treatise on Materials Science and Technology", Vol. 17 (Academic Press, New York, 1979) p. 41.
10. B. C. BUNKER, G. W. ARNOLD, E. K. BEAUCHAMP and D. E. DAY, *J. Non-Crystalline Solids* **58** (1983) 295.
11. J. HLAVAC and J. MATEJ, *Silikaty* **7** (1963) 261.
12. R. W. DOUGLAS and T. M. M. EL SHAMY, *J. Amer. Ceram. Soc.* **50** (1967) 1.
13. C. R. DAS and R. W. DOUGLAS, *Phys. Chem. Glasses* **8** (1967) 178.
14. E. GEHRKE, CH. ULLNER and M. HÄHNERT, *Glastechn. Berichte.* **63** (1990) 255.
15. T. A. MICHALSKE and B. C. BUNKER, in "Proceedings of the 7th International Congress on Fracture", Vol. 7, Houston, 1989.
16. E. GEHRKE, CH. ULLNER and M. HÄHNERT, in "Proceedings of the 15th International Congress on Glass", Leningrad, 1989, Vol. 2a, p. 269.
17. M. K. FERBER, *J. Mater. Sci.* **19** (1984) 2570.
18. H. SCHOLZE, D. H. HELMREICH, J. BAKARDJIEV, *Glastechn. Berichte* **48** (1975) 237.
19. F. M. ERNSBERGER, in "Proceedings of the 14th International Congress on Glass", New Delhi, 1986.
20. E. GEHRKE and CH. ULLNER, in "Proceedings of the 9th International Congress on Building Materials and Silicates ('ibausil')", Weimar, 1985, Vol. 4, p. 106.
21. E. GEHRKE, *Silikattechnik* **38** (1987) 10.
22. R. H. DOREMUS, Y. MEHROTA, W. A. LANFORD and C. BURMAN, *J. Mater. Sci.* **18** (1983) 612.
23. W. T. HAN and M. TOMOZAWA, *J. Amer. Ceram. Soc.* **72** (1989) 1837.
24. B. R. LAWN, D. H. ROACH and R. THOMSON, *J. Mater. Sci.* **22** (1987) 4036.
25. D. H. ROACH, S. LATHABAI and B. R. LAWN, *J. Amer. Ceram. Soc.* **71** (1988) 97.
26. B. STAVRINIDIS and D. G. HOLLOWAY, *Phys. Chem. Glasses* **24** (1983) 19.
27. A. WIGBY, *ibid.* **15** (1974) 37.
28. M. NOGAMI and M. TOMOZAWA, *J. Amer. Ceram. Soc.* **67** (1984) 151.

Received 24 July 1989
and accepted 19 February 1990